Kobe University Repository : Kernel

PDF issue: 2026-11-10

Mass and Local Topography Measurements of Itokawa by Hayabusa

Abe, Shinsuke ; Mukai, Tadashi ; Hirata, Naru ; Barnouin-Jha, Olivier S. ; Cheng, Andrew F. ; Demura, Hirohide ; Gaskell, Robert W. ;…

(Citation)
Science,312(5778):1344-1347

(Issue Date)
2006-06

(Resource Type)
journal article

(Version)
Accepted Manuscript

(URL)
https://hdl.handle.net/20.500.14094/90001254

KOBE UNIVERSITY

Mass and Local Topography Measurements of Itokawa by Hayabusa

Shinsuke Abe,[1]* Tadashi Mukai,[1] Naru Hirata,[1,3] Olivier S. Barnouin-Jha,[2] Andrew F. Cheng,[2] Hirohide Demura,[3] Robert W. Gaskell,[4] Tatsuaki Hashimoto,[5] Kensuke Hiraoka,[1] Takayuki Honda,[1] Takashi Kubota,[5] Masatoshi Matsuoka,[6] Takahide Mizuno,[5] Ryosuke Nakamura,[7] Daniel J. Scheeres,[8] Makoto Yoshikawa[5]

[1]Graduate School of Science and Technology, Kobe University, Nada, Kobe 657-8501, Japan.

[2]The Johns Hopkins University Applied Physics Laboratory, Laurel, MD 20723-6099, USA.

[3]Department of Computer Software, University of Aizu, Aizuwakamatsu, Fukushima 965-8580, Japan.

[4]Jet Propulsion Laboratory, California Institute of Technology, Pasadena, CA 91109, USA.

[5]Institute of Space and Astronautical Science, Japan Aerospace Exploration Agency, Yoshinodai, Sagamihara, Kanagawa 229-8510, Japan.

[6]NEC Aerospace Systems, Co.Ltd, Fuchu, Tokyo181-8551, Japan.

[7]National Institute of Advanced Industrial Science and Technology, Tsukuba 305-8568, Japan.

[8]Department of Aerospace Engineering, University of Michigan, Ann Arbor, MI 48109-2140, USA.

*To whom correspondence should be addressed. E-mail:

avell@kobe-u.ac.jp

Abstract

The ranging instrument aboard the Hayabusa spacecraft measured the surface topography of asteroid 25143 Itokawa and its mass. A typical rough area is similar in roughness to debris located on the interior wall of a large crater on asteroid 433 Eros suggesting a surface structure on Itokawa similar to crater ejecta on Eros. The mass of Itokawa was estimated as (3.58±0.18) x 10^{10} kg, implying a bulk density of (1.95±0.14) g/cm^3 for a volume of (1.84±0.09) x 10^7 m^3 and a bulk porosity of ~ 40%, which is similar to angular sands, when assuming an LL-type chondrite. Combined with surface observations, these data indicate that Itokawa is the first sub-km-sized small asteroid showing a rubble-pile body rather than a solid monolithic asteroid.

The LIght Detection And Ranging instrument (LIDAR) aboard the Hayabusa spacecraft, described in (*1, 2, 3, 4*), provided information on the shape and surface topography of the near-Earth asteroid 25143 Itokawa and on its mass. The LIDAR measures distance by determining the time of flight for laser light to travel from the spacecraft to the asteroid and return. The stop time measured by the LIDAR is obtained by filtering a pulse received from the surface, and measuring its time of peak intensity. In this manner, the LIDAR averages the topography within the LIDAR footprint on the surface of the asteroid, which approximates 5 x 12 m at a 7 km altitude for normal incidence. It was found that this pulse detection technique permits identifying features smaller than the LIDAR footprint.

The LIDAR operated from September 10, 2005 at a distance of 49 km from the target through November 25, a total of 4,107,104 shots were fired and 1,665,548 returns were detected. The numbers of returns reduced significantly after October 2 when spacecraft pointing was less accurate due to failures in two of the three on-board reaction wheels.

Upon arrival at Itokawa, two methods confirm the accuracy of LIDAR ranging obtained from ground calibration of the LIDAR instrument (*3*): ±1 m from a distance of 50 m and ±10 m from 50 km. In one approach, the size of the spacecraft shadow that was cast on the asteroid surface at the center of opposition point in a navigation image equaled that expected given the LIDAR-measured range measured by the spacecraft. In another approach, the height of the largest boulder on Itokawa, namely Yoshinodai, was found to be ~ 20m when using independent measurements obtained from the LIDAR and the narrow angle imager (Asteroid Multi-band Imaging CAmera; AMICA).

The LIDAR beamwidth is 0.04^{o} x 0.097^{o}, and the boresight is co-aligned with that of the near-infrared spectrometer (NIRS) with its 0.1^{o} x 0.1^{o} field of view. The NIRS alignments relative to the Hayabusa spacecraft, to AMICA, and to the wide-angle

optical navigation camera (ONC-W) used for determination of the spacecraft position relative to the asteroid (*2*), were determined from in-flight star field calibrations. The co-alignment between the LIDAR and NIRS was confirmed when NIRS detected the reflected 1064 nm Nd:YAG laser light from LIDAR (see Fig. 1), and when changes in LIDAR ranges were found to correspond with expected changes in topography seen in AMICA data.

To measure the mass of Itokawa and its surface topography, the position of the Hayabusa spacecraft relative to Itokawa must be determined. We developed a new method (Fig. 2) to estimate this spacecraft position by combining a shape model (*5*) of the asteroid determined primarily from images, ONC-W information on the direction to the center-of-light from the asteroid, and LIDAR ranging data. With these data, a first guess at the spacecraft trajectory is made. Often significant discontinuities are observed that cannot be explained by thrusting. By least squares fitting of a smooth function to the initial spacecraft trajectory, a more realistic smooth approximation is obtained, from which a cloud of LIDAR points sitting on the Itokawa surface can be determined. Checks with the actual location of the LIDAR spot in simultaneous AMICA images show that this method provides accurate spacecraft locations as well as good surface topography.

An example of the detailed surface topography that can be obtained from the LIDAR using this methodology is shown (Fig. 3) for data obtained from approximately 7 km range. In this Tsukuba area (*5*), located on the eastern side of Itokawa and representative of the rough regions on the asteroid, blocks from 3 to 10 m elevation are visible. These data contrast significantly with results obtained from the Muses Sea, that is representative of smooth regions on Itokawa (see (*6*)), where small-scale fluctuations in the elevation are observed that are comparable to the digitization of the LIDAR.

From such topographic data, the fractal roughness of the surface can be measured (*7, 8*) as the *rms* deviation σ of the height differences along a given baseline. For a 20 m baseline, which exceeds the LIDAR footprint, the Tsukuba region is characterized by a σ value of 2.2 m. This in contrast to Muses Sea where σ equals 0.6 m. Comparison of σ on Itokawa and Eros indicates that the rough Tsukuba region of Itokawa has similar roughness on 20 m baselines to that measured in the interior, near the rim, of the large crater Psyche on Eros (*8*). This region in Psyche primarily consists of disrupted materials, strewn boulders and coarse talus typical of crater ejecta. The similarity in roughness suggests that the near-surface of Itokawa resembles a rubble pile, which AMICA confirms (*1, 6*).

To investigate the interior structure of Itokawa, we also measure the mass of Itokawa in order to determine its density. We use the best data available to us that the LIDAR acquired during the rehearsal descent phase on November 11, 2005.

The Hayabusa was designed as a simple spacecraft, with fixed antennas on the upper panel perpendicular to +Z direction and fixed instruments on the base panel faced to -Z direction (to the asteroid during in-situ observations). On November 11, 2005, the Hayabusa spacecraft made a descent for the asteroid Itokawa along a Earth-Hayabusa-Itokawa line so as to do both a high rate communication with Earth and in-situ observations of the asteroid. The solar phase angle, defined as a Sun-Itokawa-Hayabusa angle, was about 8 degrees during the descent.

We estimated the acceleration term F of the spacecraft motion by using the descent data from 17:51:17 - 19:35:49 UT on November 11 (see Fig. 4A), at distances from the center of Itokawa, 1427 - 825 m. We have to subtract the effects of solar radiation pressure and thruster forces from the acceleration to estimate asteroid gravity. The thruster forces depend on injector temperature, and this contribution is presented as a

function of thruster injection rate when the maneuver uses only ± Z thrusters. The following relationship was derived from maneuver data obtained in mid-October about 10 km from Itokawa: F_{10} (cm/s^2) = 0.1603 x (thruster ratio) + 1.5695 x 10^{-5}, where thruster ratio is defined as a ratio of an integrated time of thruster burn to the total time of interest, and the acceleration due to solar radiation is calculated as 1.3303 x 10^{-5} cm/s^2.

During the above period of the descent, the thrusters were operated in only ± Z directions with a constant temperature of 35 ^{o}C, and the total number of thruster's injections was 136. Since the duration time of each thruster is 19.53 msec, the thruster ratio becomes 4.2348 x 10^{-4}, and the resulting F_{10} value is 8.3594 x 10^{-5} cm/s^2. We assumed that the acceleration caused by solar radiation force and thruster's effect is constant during the descent. As an initial condition, we subtract the above F_{10} value from the total acceleration term. Then, to investigate the gravity potential, we adopted a polyhedron method which was well suited to evaluate the gravitational field of an irregularly shaped body such as Itokawa (*9*), where we assumed a constant-density interior of the asteroid.

By fitting through least squares the spacecraft orbit during descent with calculated orbits obtained with the Itokawa's polyhedron model, we estimate the gravitational potential GM of Itokawa, where G is the gravitational constant and M denotes the mass of the asteroid (see Fig. 4B). The resulting value of GM leads to the gravitational acceleration at 10 km altitude, which is then also subtracted from the initial F_{10} to obtain an improved estimate of the solar radiation and thruster force. We then iterated the trajectory fit to the descent data to derive a revised value of GM using the modified F_{10} value and find a best estimate of GM equals to (2.39±0.12) x 10^{-9} km^3/s^2. The gravitational acceleration at the distance of 10 km from Itokawa is ~ 0.2392 x 10^{-5} cm/s^2 and it is about 3% of the acceleration term there.

Our GM value provides the mass of Itokawa of 3.58 x 10^{10} kg with an uncertainty of 5%. The shape model of Itokawa constructed using AMICA images indicates that the volume is 1.84 x 10^{7} m^3 within 5% uncertainty (*1*). Consequently, the bulk density of asteroid Itokawa measures 1.95 g/cm^3 with 7% uncertainty. Our error in mass estimation is significantly larger than that obtained by the laser rangefinder aboard the Near Earth Asteroid Rendezvous mission (*10*), because Hayabusa did not orbit the asteroid, and Eros is 190,000 times more massive than Itokawa, producing greater uncertainty in the determination of spacecraft position.

Hayabusa NIRS reported that the Itokawa spectrum near the 1-micron absorption band is similar to those of LL chondrites (*11*). Considering the bulk density of LL ordinary chondrites of 3.19 g/cm^3 (*12*), our bulk density of asteroid Itokawa indicates a high porosity of about 40% similar to that found for freshly formed coarse angular sands. Such a high porosity of Itokawa is noted in (*1*). It is known (*12*) that the porosity of five S-type asteroids studied to date does not exceed about 20%, whereas two M-type asteroids have larger porosity of about 70%, and the average porosity of four C-type asteroids is about 28%. Our porosity for Itokawa is consistent with identification as a "loosely consolidated (rubble-pile) asteroid" (*13*). Itokawa is the first S-type asteroid showing such high porosity, and the first sub-km-sized small asteroid showing a rubble-pile rather than a solid monolithic structure.

Two distinct types of terrain are found on Itokawa, rough terrain with numerous boulders and smooth terrain covered with regolith layer (*6*) which suggest a complex history, but do not predicate a heterogeneous composition. In addition, no clear regional difference in the normalized X-ray intensity ratios of Mg/Si and Al/Si has been found on the surface of asteroid Itokawa (*14*), indicating homogeneous composition. NIRS reported olivine-rich mineral assemblages similar to LL5 and LL6 chondrites, with variations in albedo and absorption band depth more than 10%, but this diversity may be consistent with differences in freshness and/or particle size (*11*), and it does not suggest the presence of unusual inhomogeneous materials.

As noted in (*15, 16*), the size of asteroid, 150 - 1000 m in radius, may be a transition size between monolithic structure and rubble pile structure. The large porosity of ~ 40% and the roughness of the surface found on Itokawa strongly suggest a rubble pile structure. The 12.1324 hours spin period of Itokawa (*1*) is far above the critical value of 2 hours, where a rubble pile structure cannot be withstand centrifugal forces [e.g. (*17*)], and is also consistent with a rubble pile structure.

The internal structure of the asteroid Itokawa gives us a hint of its origin. It is predicted based on the numerical simulation of orbital evolution of asteroid Itokawa that the most probable source region of asteroid Itokawa is the inner part of the main belt (*18*). High porosity in asteroid Itokawa may be the result of gravitational aggregation of the collision fragments.

References and Notes

1. A. Fujiwara *et al*., *Science*, (2006); this issue
2. T. Hashimoto, T. Kubota, T. Mizuno, *Acta Astronautica* **52**, 381 (2003).
3. T. Mukai *et al*., *Adv. Space Res*. **29**, 1231 (2002).
4. T. Mukai *et*, A. M. Nakamura, T. Sakai, *Adv. Space Res*. **37**, 138. (2006).
5. H. Demura *et al.*, *Science*, (2006); this issue
6. J. Saito *et al*., *Science*, (2006); this issue
7. A. F. Cheng *et al.*, *Science* **292**, 488 (2001).
8. A. F. Cheng *et al.*, *Icarus* **155**, 51 (2002).
9. R. A. Werner, D. J. Scheeres, *Celestial Mechanics and Dynamical Astron*. **65**, 313 (1997).
10. M. T. Zuber, D. E. Smith, A. F. Cheng, J. Garvin, *et al.*, *Science* **289**, 2097 (2000).
11. M. Abe *et al*., *Science*, (2006); this issue
12. D. T. Britt, D. Yeomans, K. Housen, G. Consolmagno *in Asteroids III.* (Univ. of Arizona Press, Tucson, AZ, 2002), p.485.
13. D. C. Richardson, Z. M. Leinhardt, H. J. Melosh, W. F. Bottke Jr., E. Asphaug *in Asteroids III.* (Univ. of Arizona Press, Tucson, AZ, 2002), p.501.
14. T. Okada *et al*., *Science*, (2006); this issue
15. W. Benz, E. Asphaug, *Icarus* **142**, 5 (1999).
16. E. Asphaug, E. V. Ryan, M. T. Zuber, *Asteroids III.* (Univ. of Arizona Press, Tucson, AZ, 2002), p.463.
17. P. Pravec, A. W. Harris, T. Michalowski *in Asteroids III.* (Univ. of Arizona Press, Tucson, AZ, 2002), p.113.
18. P. Michel, M. Yoshikawa, *Astron. Astrophys.* **449**, 817 (2006).

19. Supported by ISAS/JAXA through the Hayabusa mission. We are extremely grateful for the numerous engineers and supporting scientists who were critical to the successful development and execution of the first mission rendezvoused and landed on an asteroid. We thank E. Okumura and K. Tsuno (NEC TOSHIBA Space Systems, Ltd.) for their great efforts to develop the LIDAR. This work is partly supported by the 21st Century COE Program "Origin and Evolution of Planetary Systems" under the MEXT.

Figure captions

Fig. 1. LIDAR spectrum observed by NIRS. The 0.1^o x 0.1^o square shaped field of view of NIRS was co-aligned with that of LIDAR (a 0.04^o x 0.097^o ellipse). LIDAR spectra reflected by Itokawa were detected by NIRS during the decent. Figure shows a LIDAR spectrum obtained by NIRS from an altitude of 900 m at 01:02:22 UT on November 12, 2005. Dotted line indicates observed LIDAR spectrum after subtracting a spectrum of the asteroid Itokawa. A pre-flight spectrum of LIDAR measured by NIRS is shown as a solid line for comparison with the one measured in flight. NIRS has a 64-channel InGaAs photodiode array detector corresponding to 764 - 2248 nm which includes the reflected 1064 nm Nd:YAG laser light from LIDAR. The LIDAR signal detected by NIRS confirmed that LIDAR and NIRS instruments were co-alignment within the field of view accuracy, i.e., 1.7 m at a distance of 1 km.

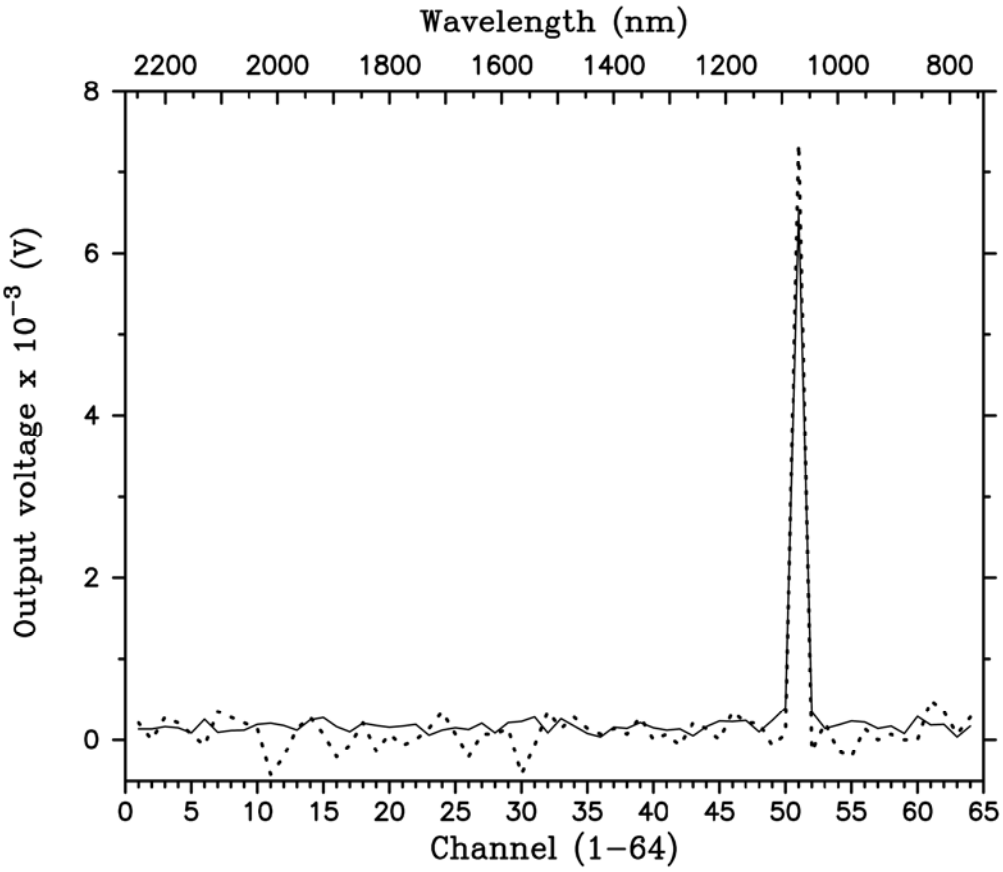

Fig. 2. Conceptual drawings of the method to estimate the position of the spacecraft (S/C). (**a**) ONC-W takes images of the asteroid every 128 seconds, and the onboard computer calculates the center of light (COL) of the asteroid image. The pixel coordination of COL in the camera detector is included in the telemetry. (**b**) With a shape model of the asteroid determined primarily from images (although any approximate shape model can be used), an artificial camera image of the asteroid is simulated. Even though this image is non-scaled, two vectors from the S/C to COL and to the shape/mass center (COM) of the asteroid are obtained. (**c**) From COM information and the simulated image, the location of the asteroid relative to the S/C is estimated with one degree of freedom on a line along the S/C-COM vector. Finally, the distance to the asteroid is obtained from an actual ranging data of LIDAR and the shape model. Through iterations, a very accurate spacecraft location can be found. This procedure was carried out on all pairs of the LIDAR ranging data and COL telemetry.

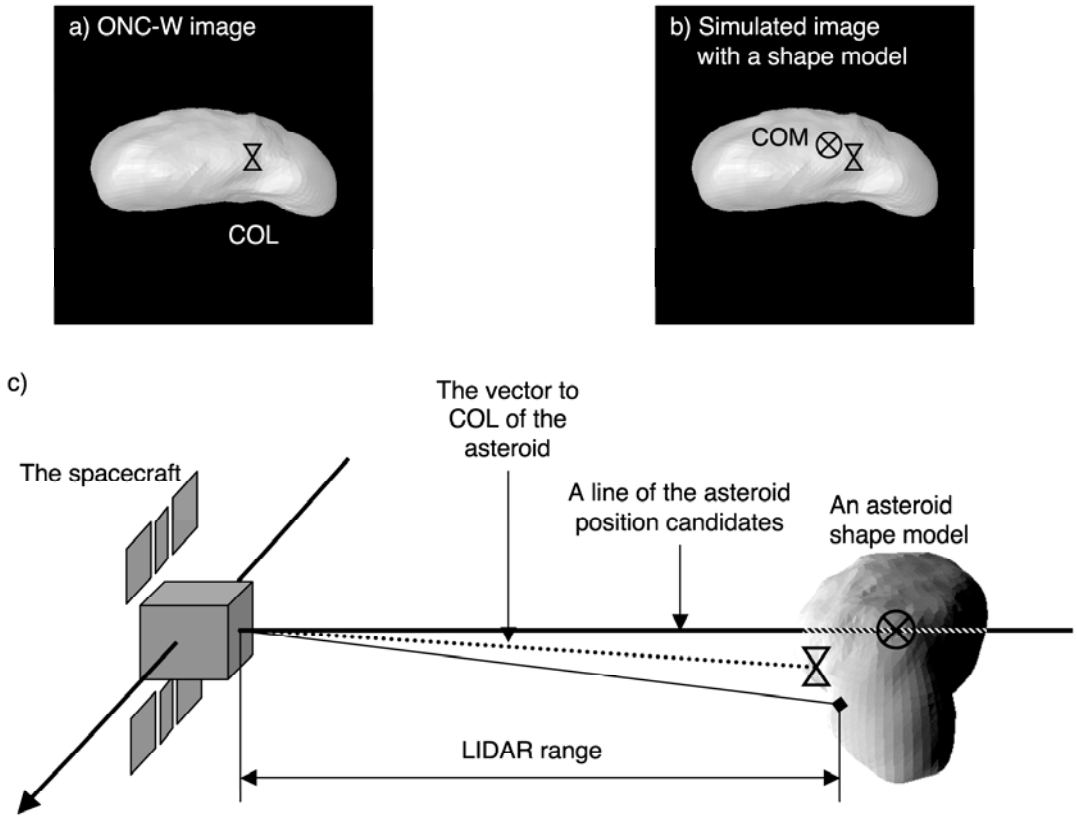

Fig. 3. Location and elevation of LIDAR spot near Tsukuba region. (**a**) AMICA image ST_2420994934 showing 17 predicted locations of LIDAR spot; (**b**) simple cylindrical projection of the transect in meters North and East; (**c**) relative elevation (m) along the LIDAR profile where the distance along the path is measured along the transect as if it were completely unwound. This elevation *e* is computed relative to a reference geoid as done in (*7, 8*): a ball would roll downhill from a high *e* to low *e.* The digitization error in these data is about ±1.5 m. Data points in (b) are color-coded by relative elevation according to (c). The letters in the lower two panels correspond to the circles seen in (a) going right to left. Panels (a) and (b) show how the location of the LIDAR spot fluctuates with time due to spacecraft pointing oscillations discussed in the text. Blocks with about 3-4m elevation and the horizontal size of the order of the LIDAR spot are shown as sudden increases in elevation at locations D and G in panel (c). A jump at point J seen in elevation of about 5 m and 10-15 m horizontally, corresponds to the central Tsukuba feature in (a).

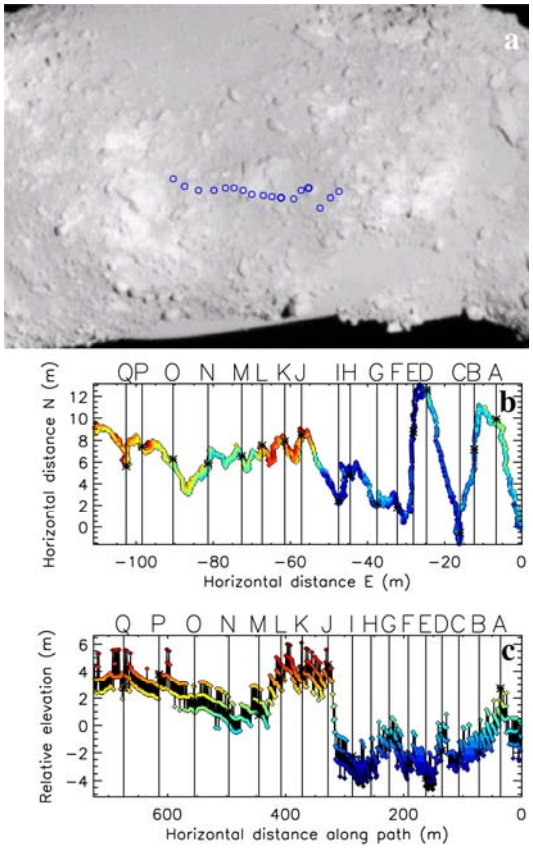
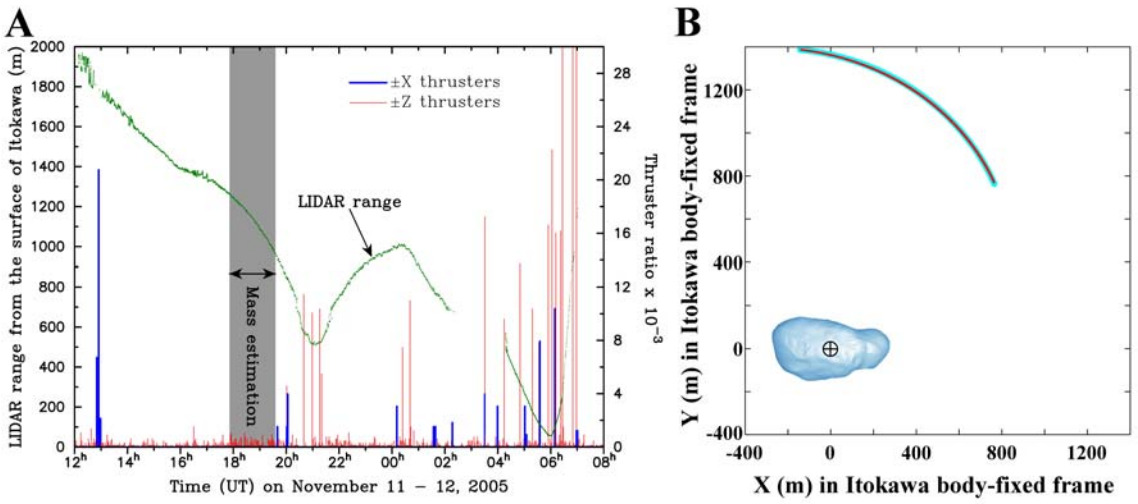
Fig. 4. (**A**) LIDAR range and thruster ratio during the rehearsal decent of November 11, 2005. LIDAR missed the surface during 2:20 - 4:17 UT. The period of 105 minutes for the mass estimation shows no abrupt changes and is very smooth relative to the other periods, and moreover the effect of thrusters in the direction of ± Z could be accurately estimated. (**B**) The position of the Hayabusa spacecraft relative to its computed trajectory. The position of Hayabusa in body-fixed frame(thick sky-blue curve) was determined by LIDAR ranging data with images of the wide-angle optical navigation camera (ONC-W) as described in the text. This approach phase has a good opportunity to measure the gravitational field because the gravitational acceleration of Itokawa is about 18 times stronger than the acceleration due to solar radiation pressure at the distance of 1 km from Itokawa. The red curve on the thick sky-blue curve shows the computed trajectory of the Hayabusa spacecraft for the best fitted GM of 2.39 x 10^{-9} km^3/s^2. The adopted shape model (5) for this computation is shown, which ellipsoidal diameters are 535(X) x 294(Y) x 209(Z) m, respectively.